Dalton Transactions

PAPER

View Article Online
View Journal

Cite this: DOI: 10.1039/c9dt02080b

Azamacrocycles and tertiary amines can be used to form size tuneable hollow structures or monodisperse oxide nanoparticles depending on the 'M' source†‡

Graham E. Tilbury,[a] Toby J. Blundell,[b] Stephen P. Argent[c] and Carole C. Perry *[a]

We show that the azamacrocycle 'cyclam' (1,4,8,11-tetraazacyclodecane) in conjunction with a silicon catecholate ion generates novel hollow tetragonal tube-like crystalline materials $[(C_6H_4O_2)_3Si][C_{10}H_{26}N_4]\cdot H_2O$, whose dimensions can be tuned according to the pH of the reaction medium. The synthesis approach was successful for both silicon and germanium and we hypothesise that a range of other catecholate precursors of elements such as iron could be used to generate a large array of inorganic materials with interesting morphologies. The synthesis approach can be extended to tertiary diamines with functional group spacing playing an important role in the efficacy of complexation. Of the molecules explored to date, a C2 spacing (*N*,*N*,*N*′,*N*′-tetramethylethylenediamine (4MEDAE)), leads to the most efficient structure control with hollow hexagonal tube-like structures being formed. In addition, we show that azamacrocycles, in the presence of unbuffered tetramethoxysilane (TMOS) solutions can be used to manipulate silica formation and provide a fast (*ca.* 10 minutes) synthesis route to particles whose diameter can be tuned from *ca.* 20 nm to several hundreds of nm under reaction conditions (no extremes of pH) that make the sols suitable for direct use in biotechnological applications.

Received 17th May 2019,
Accepted 24th June 2019

DOI: 10.1039/c9dt02080b

rsc.li/dalton

Introduction

The ability of azamacrocycles to bind to transition metal and lanthanide ions forming thermodynamically stable complexes[1–3] has led to the development of a new generation of abiotic host molecules that contain a signalling or responsive functional group enabling the development of molecular sensors.[1,2] The chelation of Gd(III) by azamacrocycles gives molecular species that can be used as contrast agents in magnetic resonance imaging (MRI), where strong binding of the metal and occupation of most of the available coordination sites is vital.[4] Cyclam, (1,4,8,11-tetraazacyclotetradecane) and related compounds have been used in the preparation of new inorganic–organic hybrid materials such as gallium phosphates,[5,6] novel microporous aluminophosphates[7] and magnesioaluminophosphates.[8] Interestingly, azamacrocycles have been found to interact with the crystallising inorganic framework in two different ways.[8–11] The first is found in gallium phosphate hybrid materials where cyclam was found to be covalently bonded to the zeolite-like gallium phosphate framework.[9] This structure permits metal cation exchange with other ions forming stronger complexes with the macrocycle, such as Cu^{2+}.[9] This type of interaction was found in metalloaluminophosphates where the azamacrocyclic molecule, 1,4,8,11 tetramethyl 1,4,8,11-tetraazacyclodecane (4MC) was found to act as a structure directing agent around which the inorganic framework crystallises forming STA-6, 7 and 8 structures depending on the metal cation present.[8,10,11] A further example is where the azamacrocyclic molecule is present in the crystal structure of the material, but does not coordinate a metal ion. Gallium in the presence of 1,4,7,10,13,16-hexaazacyclooctadecane is one such example where the gallium ion is too small to be effectively coordinated to the azamacrocyclic molecule resulting in the azamacrocyclic molecule being present in pores within the structure and not bound to the framework.[12]

Molecular self-assembly has become one of the fastest growing areas of research in materials chemistry over the past few decades, leading to the production of biologically inspired nanomaterials.[13] One such area of research is the formation of

[a]*Biomolecular and Materials Interface Research Group, Interdisciplinary Biomedical Research Centre, Nottingham Trent University, Clifton Lane, Nottingham NG11 8NS, UK. E-mail: carole.perry@ntu.ac.uk*
[b]*Department of Chemistry and Forensics, Nottingham Trent University, Clifton Lane, Nottingham NG11 8NS, UK*
[c]*School of Chemistry, University of Nottingham, University Park, Nottingham NG7 2RD, UK*

† In honour of the 60th birthday celebrations of Professor Annie Powell.

‡ Electronic supplementary information (ESI) available. CCDC 1916071. For ESI and crystallographic data in CIF or other electronic format see DOI: 10.1039/c9dt02080b

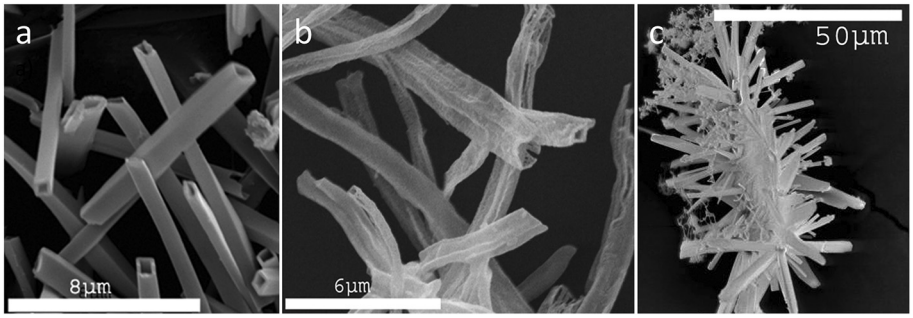

Fig. 1 SEM images of (a) tetragonal tubes, prepared from potassium silicon catecholate and cyclam at a Si : N ratio of 10 : 1 (b) tetragonal tubes from (a) after heat treatment to 900 °C, and (c) structures generated at a Si : N ratio of 2 : 1 showing multiple nucleation sites.

bioinspired nano-patterned silica materials where inspiration has been taken from silica accumulating organisms such as diatoms,[14] sponges and higher plants.[15] Extensive studies of silica formation have been performed using biomolecule isolates (proteins and long chain polyamines) as well as simpler chemical mimics such as amino acids, peptides and amines.[16,17] Importantly, in the context of the present contribution, self-assembly of the organic moiety has proved important in the generation of structurally organised amorphous silicas.[18] Molecular architecture has a significant effect on the catalytic ability and morphological control exerted by (bio) molecules on the formation of silica *in vitro*.[19–21] Additives ranging from polyelectrolytes to small molecules having a significant effect on silica formation *in vitro* either catalytically or through molecular templating usually contain some degree of amine functionality.[16,22] Complex structures which have been generated include: hollow spheres formed in the presence of long chain polyamines,[23] amorphous silica hexagonal plates formed in the presence of alpha-helical arrays of polylysine,[24,25] hollow nano-fibres,[26] silica tubes[27] and hybrid organic–inorganic amorphous tubes.[28]

In this contribution we investigate the effect of amine molecular architecture on the formation of novel silica morphologies. Further, the unique ability of azamacrocyclic molecules to interact with chemical species to generate crystalline solids lead to the hypothesis that they might also interact with a forming amorphous inorganic material such as silica. We present the results of interaction studies with two different silicic acid precursors, namely tetramethoxysilane (TMOS), that is commonly used in biomimetic studies of silica formation and potassium silicon catecholate (KSicat) where the silicon is octahedrally coordinated and relatively 'high' concentrations of monomeric silicon species can be maintained in solution. Specifically we show that according to the precursor used cyclam can be used to induce the formation of a novel layered crystalline structure in the form of hollow tetragonal needles (KSicat as precursor) or tune the sizes of silica sols at the tens of nm level (TMOS precursor). Further, tertiary amines with a range of functional group spacings can also be used to generate macroscopic ordered silicon catecholate : diamine complexes and a range of azamacrocycles with a minimum of 14 ring atoms can be used to tune the sizes of silica particles from *ca.* 20–800 nm (TMOS precursor).

Results and discussion

A range of aza- and oxo-compounds having C2 or C3 spacing between the functional groups were tested for their ability to interact with an aqueous solution containing potassium

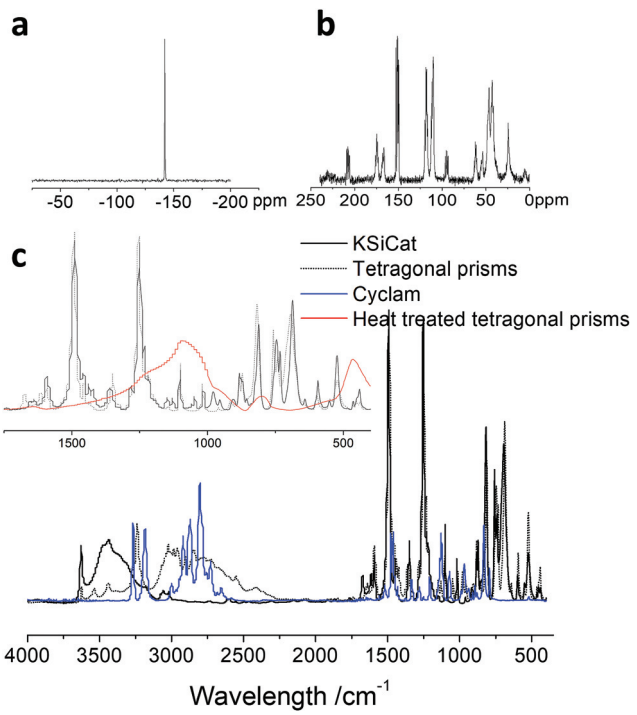

Fig. 2 NMR and FTIR characterisation of hollow tubes formed from the reaction between potassium silicon catecholate at a Si : N ratio of 1 : 1. (a) 29-Si solid state nmr, CP-MAS, (b) 13-C solid state nmr, CPMAS, and (c) FTIR spectra of tetragonal prism, KSiCat and cyclam, insert shows close up of 1750–450 cm^{-1} where the Si–O peak at 1100 cm^{-1} is retained from KSiCat in the tetragonal prisms. Upon heat treatment the Si–O stretch is broad showing the presence of amorphous silica.

silicon catecholate (see Materials section with images shown in ESI1‡). Novel macroscopic structures (needles) formed in the presence of 1,4,8,11-tetraazacyclodecane (cyclam) only.

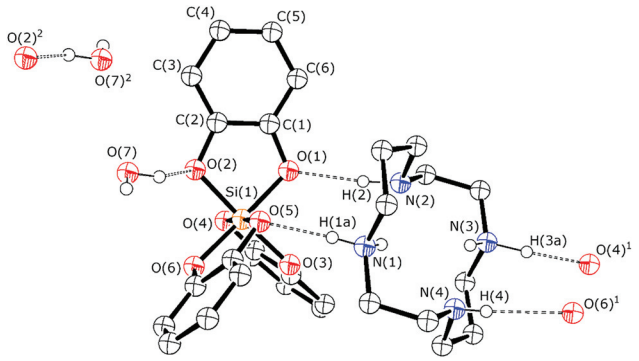

Fig. 3 Asymmetric unit of $[(C_6H_4O_2)_3Si][C_{10}H_{26}N_4]\cdot H_2O$ with labelling scheme. Thermal ellipsoids set at 50% probability; some hydrogen atoms omitted for clarity. Symmetry operations: [1] $-1 + x, y, z$, [2] $2 - x, 1 - y, 2 - z$.

Hollow rod-like structures (needles) formed almost immediately on mixing at a molar range of 10 : 1 for Si : N with the purest samples being formed by around 60 minutes after mixing, Fig. 1a. Typical yields were *ca.* 90%+ based on the amount of cyclam present, ESI2.‡ If samples were left considerably longer than this then samples containing both needles and other less ordered material formed, ESI3.‡ EDXA analysis of the different material types showed that the needles contained Si, C, N and O, ESI4.‡ No K was detected in the rod-like structures, ESI4.‡ Treatment of structurally mixed samples with acid (2 M HCl) destroyed the tube-like structures but not the unordered materials giving further evidence that the two were different in chemical composition and structure.

Material isolated at *ca.* 60 minutes after mixing yielded material that was principally rod-like, Fig. 1a and was used for further analysis by solid state NMR, FTIR, TGA and X-ray diffraction (single crystal and powder). The temperature profile of the TGA analysis of the rod-like structures was also used to generate structures retaining the rod-like shape and consisting of material that was resistant to heat treatment at 900 °C, Fig. 1b and ESI6.‡

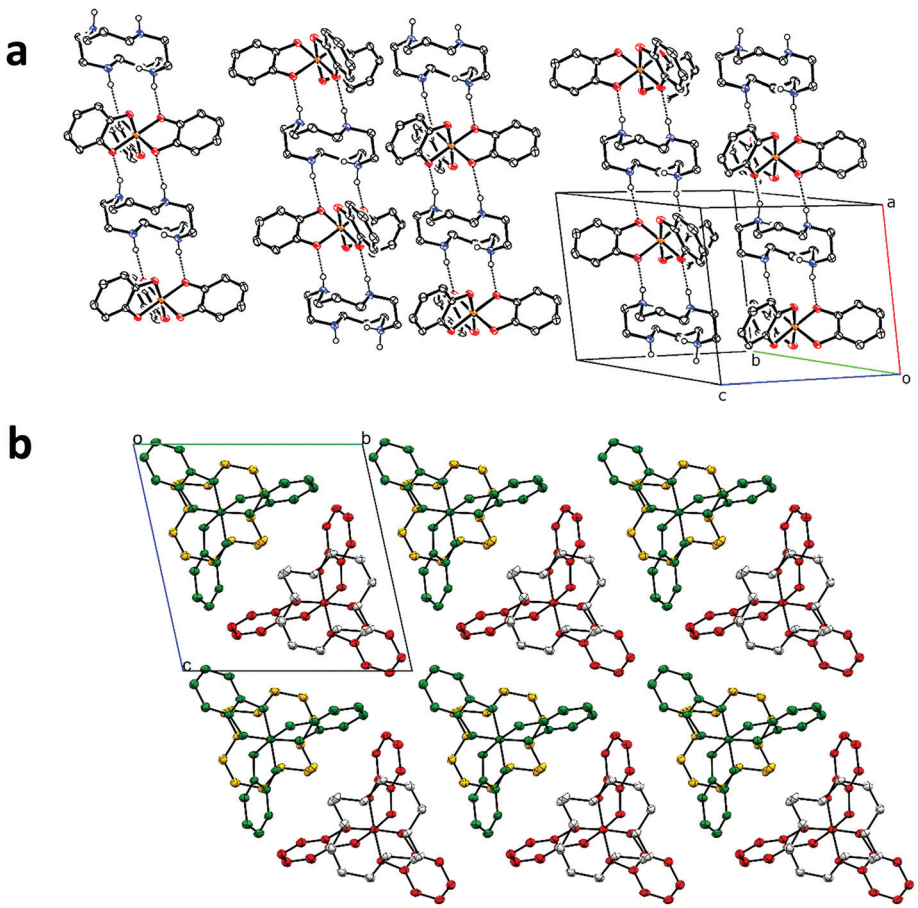

Fig. 4 a. Crystal packing of $[(C_6H_4O_2)_3Si][C_{10}H_{26}N_4]\cdot H_2O$ showing hydrogen bond network (dashed lines), top. C – black, O – Red, N – Blue, Si – Orange, H – White. b. Crystal packing viewed down the crystallographic *a* axis showing layers of the two chiral enantiomers of $[(C_6H_4O_2)_3Si]^{2-}$ Λ – Red, Δ – Green. Cyclam white and yellow for the respective layers. Thermal ellipsoids set at 50% probability; some hydrogen atoms omitted for clarity.

Solid state NMR of 'pure' samples of the tetragonal prisms was used to confirm the presence of silicon in an octahedrally coordinated environment (single peak at 142 ppm) and the presence of both catechol and cyclam in the structure, Fig. 2a and b. ^{13}C NMR shows characteristic peaks of aromatic carbon atoms in the same positions as the starting precursor dipotassium tris(1,2-benzenediolato-*O*,*O*′) silicate at 111, 150 and 180 ppm, and the peaks at 24, 42 and 46 ppm can be assigned to cyclam which have been shifted to slightly lower ppm values suggesting the involvement of hydrogen bonding in the tetragonal prisms. Thermogravimetric analysis coupled with CHN analysis was used to confirm the composition of the needle-like phase, where the needles were suggested to contain a *ca.* 1 : 1 ratio of the silicon catecholate and cyclam, see ESI5‡ for data and calculation. The lack of difference between the thermogram collected on samples isolated at 5 minutes or 60 minutes after mixing further suggests that the needles once formed do not interact further with any residual silicon containing species in solution, ESI6.‡

FTIR analysis of the material as prepared, contained signatures of both the cyclam and the Sicat complex, Fig. 2c. The FTIR spectra contain two distinct regions; region 1 from 4000–2250 cm^{-1} and region 2; 1750–400 cm^{-1}. Region 1 for the rod-like structures included a secondary N–H stretching band centred at *ca.* 3200 cm^{-1} and a loss of the O–H stretch at *ca.* 3500 cm^{-1} suggesting that water in the native KSiCat salt is largely replaced by cyclam in the structures formed. Region 2 showed only slight differences with the peaks shifted to slightly higher wavenumbers in the tetragonal prisms. The characteristic peaks at *ca.* 1500, 1250 and 1100 cm^{-1} attributed to substituted aromatic molecules, the aryl =C–O and the Si–O stretch respectively, all appear in both spectra indicating the presence of tris(1,2-benzenediolato-*O*,*O*′)silicate (SiCat). The Si–O band appears narrow in both the tetragonal prisms and in KSiCat indicating that the Si–O bonds are in similar environments and since the peak has not shifted in the tetragonal prisms when compared to KSiCat we suggest that the silicon atoms remain octahedrally coordinated. After heat treatment of the tetragonal prisms (Fig. 2c insert) the Si–O band at 1100 cm^{-1} appears broad, characteristic of the Si–O–Si antisymmetric stretching vibrations of amorphous silica as well as a peak at 805 cm^{-1} of symmetric Si–O–Si stretching. Small differences in the fingerprint region suggest that the Sicat complex remained intact within the structure.

The data obtained by FTIR, ^{29}Si NMR and TGA provide evidence that the tetragonal prisms are a complex formed between undissociated SiCat and cyclam, where the tetragonal prism morphology is assumed to form by molecular self-assembly. Evidence for the assembly was gained from single crystal X-ray analysis of the needle-like crystals. $[(C_6H_4O_2)_3Si][C_{10}H_{26}N_4]\cdot H_2O$ crystallises in the triclinic crystal system in the centrosymmetric space group $P\bar{1}$. The asymmetric unit consists of one slightly distorted octahedral silicon(IV) atom coordinated by three catechol ligands as well as one doubly protonated cyclam and one water molecule (Fig. 3).

A network of hydrogen bonds exists between the oxygens on the catechol ligands and the nitrogen atoms of the cyclam (Fig. 4a, Table 1). Due to the centrosymmetric nature of the unit cell two chiral enantiomers (delta and lambda) of the silicate are present in the structure (Fig. 4b).

The Si–O bond lengths (range 1.7775(11) Å for Si(1)–O(3) to 1.7983(11) Å for Si(1)–O(2)) and angles (O(1)–Si(1)–O(2) 88.21(5)°, O(3)–Si(1)–O(4) 88.89(5)°, and O(6)–Si(1)–O(5) 88.23(5)°) are similar to that of the analogous amine containing silicates $[C_3H_7NH_3]_2[Si(C_6H_4O_2)_3]\cdot 0.5(C_6H_{14}N_2)$,[29] and $[(C_6H_4O_2)_3Si][\{((CH_3)_2CH\}_2NH_2]_2\cdot 2(CH_3CN)(H_2O)$[30] (Si–O1 – 1.791(3) Å, Si–O(2) – 1.808(3) Å, Si–O(3) – 1.766(3) Å, Si–O(4) – 1.791(3) Å,

Table 1 Table of relevant hydrogen bond lengths and angles. Symmetry operation * = 1 + *x*, *y*, *z*

N–O distance	N–O length (esd) Å	N–H distance Å (angle °)
N(1)–O(5)	2.7551(17)	1.946 (169.76)
N(2)–O(1)	2.9843(17)	2.029 (172.40)
O(6)–N(4)*	3.0043(16)	2.095 (171.19)
O(4)–N(3)*	2.7680(16)	1.778 (162.21)
O(2)–O(7) [O(2)–H(7B)]	2.712(2) [2.0278]	

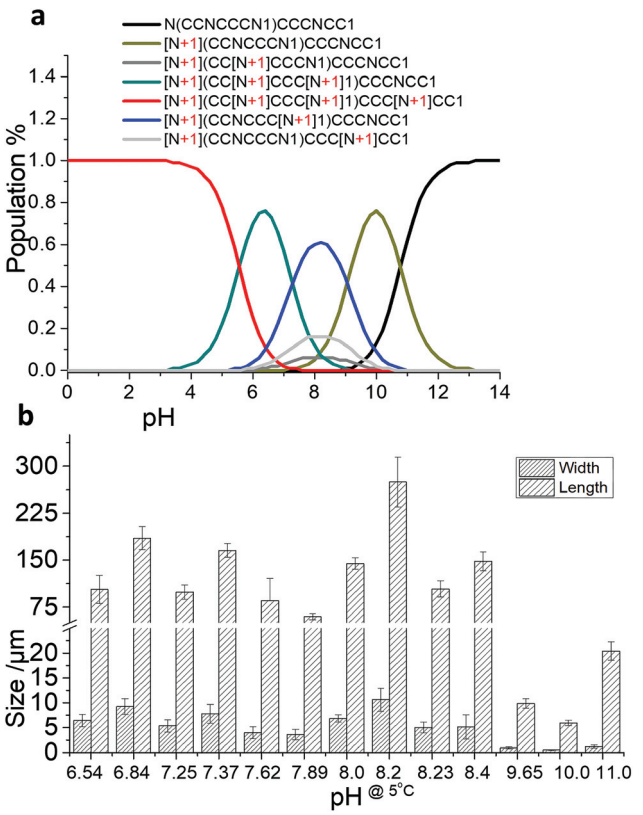

Fig. 5 (a) Speciation diagram for cyclam calculated used SPARC.[32] It is known that cyclam exhibits an unusual speciation where protonation of the fourth amine requires less energy than the third[33] and as such the calculated speciation diagram from SPARC was only used as a guide. (b) pH range over which needles were formed and their sizes. A minimum of 13 needles were measured for each sample.

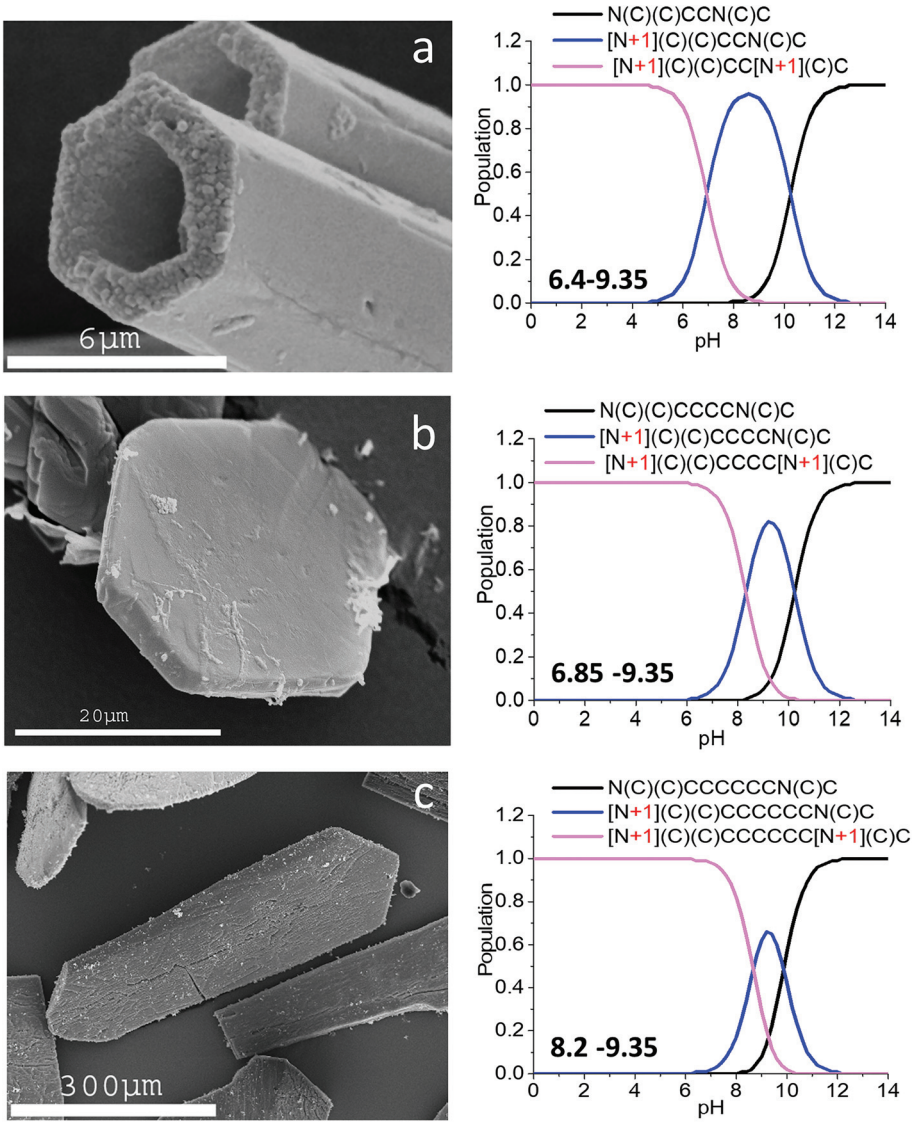

Fig. 6 Representative SEM images of organised structures formed in the presence of (a) 4MEDAE, (b) 4MEDAB and (c) 4MEDAH together with speciation diagrams generated using SPARC pK_a calculator.[32] The pH range over which organised structures form is indicated for each system.

Si–O(5) – 1.783(3) Å, Si–O(6) – 1.780(3) Å, O(1)–Si–O(2) – 87.53(13)°, O(3)–Si–O(4) – 88.58(14)° and O(5)–Si–O(6) – 88.41(13)°) and the bis-ethylaminediamine copper containing $[(C_6H_4O_2)_3Si]$ $[Cu(C_2H_8N_2)_2]$[31] (Si–O – 1.778–1.809 Å, O–Si–O – 88.3–89.3°). The silicon atom is in a slightly distorted octahedral arrangement where the angles of the O–Si–O of each catechol deviate slightly from the idealised 90°. Each chelating catechol ligand forms two bonds to silicon *via* the oxygen atoms (Fig. 3). A single water molecule is present forming a hydrogen bond with the oxygen atom of one of the catechols (O(2)–O(7) – 2.712(2) Å, O(2)–H(7a) 2.0278 Å).

The structure consists of distinct layers or sheets of silicate and cyclam molecules along the crystallographic *b*/*c* axes, with a hydrogen bond network between the cyclam and silicate molecules of individual layers. Each layer contains only a single enantiomer of the chiral silicate with the layers alternating between Λ and Δ (Fig. 4b).

A hydrogen bond network exists along the crystallographic a axis between the cyclam N–H and catechol oxygen atoms as follows: the hydrogen atoms on N(1) and N(2) form hydrogen bonds with O(5) and O(1) respectively of the catecholate. O(4) and O(6) are hydrogen bond acceptors for the other two cyclam nitrogen atoms (N(3) and N(4) respectively) completing the one-dimensional hydrogen bond network that permeates through the solid-state structure (Fig. 4a, bond lengths and hydrogen bond angles in Table 1). That similar structures are not formed between 1,8-dimethyl 1,4,8,11-tetraazacyclodecane (2MC) and the silicon catecholate even though the doubly charged protonation state for the amine is possible suggests that it is principally sterics that preclude the formation of such materials.

The coordination pattern for the azamacrocycle cyclam is unlike that previously reported for azamacrocycle containing compounds where either covalent bonds were formed between species[9] or the macrocycle was situated in pores[12] and thus the structure described above represents a new coordination pattern.

Needles could be formed at a range of pH values, the success of which could be explained by considering the charge state of both the catecholate and the azamacrocyclic with success being achieved provided the catecholate salt was stable (pH > 6.5) and the azamacrocyclic contained at least one, and preferably two positive charges, Fig. 5.

Both pH and the Si : N ratio affected the structure of the macroscopic materials formed. Tetragonal prisms, though differing in aspect ratio could be formed over the pH range (6.54–11.00), Fig. 5b that correlated with ability of the macrocycle to carry one or two positive charges, Fig. 5a as well as being above the pH at which the silicon catecholate salt was stable. Decreasing the Si : N ratio from 10 : 1 through to 2 : 1 did not improve the yield of rod-like materials with stars and other aggregated structures being formed, Fig. 1c.

The formation and characterisation of tetragonal prisms using dipotassium tris(1,2-benzenediolato-*O*,*O*′)germanate

We tested the generality of the approach using dipotassium tris(1,2-benzenediolato-*O*,*O*′)germanate (KGeCat). In this case base was added to the KGeCat solution to provide a range of pH values compatible with the different protonation states of cyclam. Hollow tetragonal prisms (*ca.* 30 × 3 microns-smaller than for Si) were formed over a wide pH range (6.7–11.4) whose X-ray powder diffraction pattern was very similar to that generated for the Si based materials, ESI8 and SI10.‡

The precipitation of tris(1,2-benzenediolato-*O*,*O*′)silicate complexes using tertiary amines

Although only one of the azamacrocylic compounds formed a crystalline complex with silicon catecholate ions we tested a range of diamines containing primary, secondary and tertiary amine functionality at a Si : N ratio of 1 : 1 at pH 6.8 ± 0.2 as per the compounds listed in the materials and methods section. Addition of tertiary amines led to the formation of complex structures comprising the amine and the silicon catecholate. The role of functional group spacing on the structures formed was investigated using the tertiary diaminoalkanes with 2, 4 and 6 carbon atoms between the amine groups namely; *N*,*N*,*N*′,*N*′-tetramethylethylenediamine (4MEDAE), *N*,*N*,*N*′,*N*′-tetramethyl-1,4-butanediamine (4MEDAB) and *N*,*N*,*N*′,*N*′-tetramethyl-1,6-hexanediamine (4MEDAH). Images of typical structures formed, the pH range and the speciation of the diamines as estimated using SPARC is presented in Fig. 6. The pH range over which organised structures formed decreased as the number of carbon atoms between the amine groups was increased corresponding to the reduced pH range over which charge was carried by the amine.

Unlike the experiments conducted with cyclam, structures formed in the presence of *N*,*N*,*N*′,*N*′-tetramethylethylenediamine (4MEDAE) showed a high dependency on the pH of the solution. Needle-like hollow hexagonal rods formed from pH 6.85 and for experiments performed at pH 8.5, hexagonal rods were formed. Experiments conducted at intermediate pH values (*i.e.* 8.21 showed a capping of the hollow rods. Example SEM images of the structures formed can be found in ESI9.‡

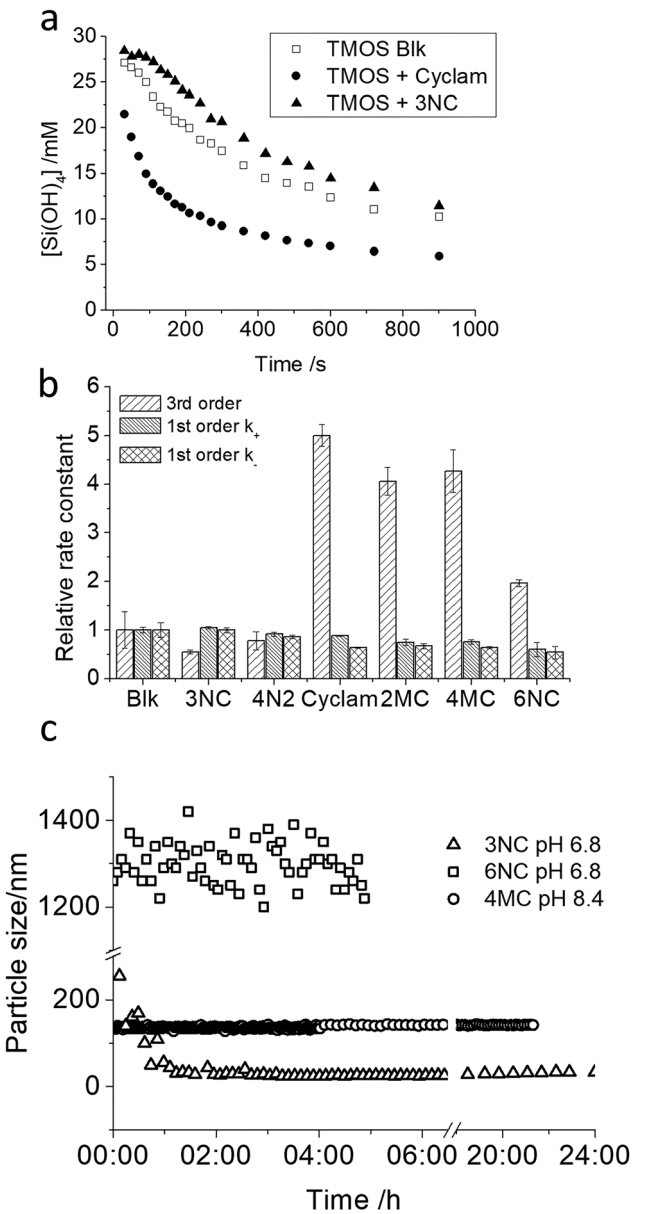

Fig. 7 Reaction of hydrolysed TMOS in the presence of a range of azamacrocycles at pH 6.8. (a) Raw data from a molybdenum blue assay Si : N = 10.1 showing amount of orthosilicic acid left in solution after reaction times in seconds, (b) kinetic rate constants for the early stages of silica formation in the presence of azamacrocycles at a Si : N ratio of 10 : 1, (c) exemplar DLS data showing particle size *versus* time. The data show a rapid stabilisation of structures at a range of sizes from TMOS with Si : N ratio of 1 : 1. Details on the specific azamacrocycles used is given in ESI1.‡

Characterisation of the materials formed showed that similarly to the cyclam silicon catecholate complexes, EDX confirmed the absence of metal cations, FTIR confirmed the presence of both the amine and the silicon catecholate salt, and powder XRD traces were similar to those obtained for the cyclam-silicon catecholate material, see ESI9.‡ TGA of the hexagonal rods formed at pH 8.51 showed that 88% of the materials mass is lost upon heating to 900 °C of which 37% can be attributed to organic material lost between 400 and 650 °C. Silica only replicates of the initial structure could be generated but it was not possible to obtain single crystal X-ray diffraction data to confirm the local environment of the two ionic components. Based on the pH range over which complexation occurred and assuming the mechanism for complex formation is similar to the that exhibited by cyclam then it would seem likely that the $[4MEDAE]^+$ species is involved. If the coordination pattern is similar to that encountered between cyclam and the silicon catecholate ion then we would expect two amine molecules to complex with one silicon catecholate ion.

Addition of a further two or four $-CH_2$ groups between the amine groups 4MEDAB and 6MEDAH led to the formation of hexagonal plates (4MEDAB) or samples that contained both disordered material and particulate sheets (6MEDAH), Fig. 6 that although containing both the silicon catecholate ion and the amine (evidence from FTIR ESI9‡) were not stable to extensive washing. Further, the pH range over which such structures formed decreased in line with the amine speciation changes predicted by SPARC. We hypothesise that the structures observed contain both the amine and the silicon catecholate ion though it is clear that as the spacing of the two amines increases the ability to form stable structures decreases markedly, perhaps due to steric constraints.

Using azamacrocyles to generate monodisperse silica sols

Although only cyclam was able to form a structural complex with the silicon/germanium catecholate salt a number of azamacrocycles impacted silica formation, both in the early stages of condensation and in the stabilization of mono-disperse sols when the silicon precursor was changed to unbuffered TMOS at an Si : N ratio of 1 : 1, we found that azamacrocycles were generally very good at catalysing silica formation, Fig. 7a. There was an optimum ring size (14 atoms) for acceleration of the initial stages of condensation Fig. 7b. Dynamic light scattering was used to investigate the rates of aggregation of silica with a range of stable sols being formed in the presence of azamacrocycles, Fig. 7c. The materials that were isolated when either cyclam, 2MC or 4MC were the additives were essentially silica with low levels of entrapped organic material (*ca.* 2%), data not shown. The material isolated after additions of 6NC was somewhat different as it contained *ca.* 10% entrapped organic material, data not shown.

The effect of pH on silica particle size using the azamacrocyclic molecules was investigated using the unbuffered TMOS system, Fig. 8. Initial results show that the stabilised particle size is dependent on the pH of the solution and the azamacrocyclic molecule used. According to the azamacrocyclic used a range of stable sols can be formed from 65–115 nm (cyclam); 105–300 nm (2MC), 30–210 nm (4MC) and 250–750 nm (6NC). The mechanism of stabilisation is currently unknown but a suggested pathway may involve phase separation and droplet formation of the amine containing molecule as previously encountered for silica formation in the presence of polyamines,[23,33] alternatively, the azamacrocyles could act to cap the silica materials once formed though this is unlikely

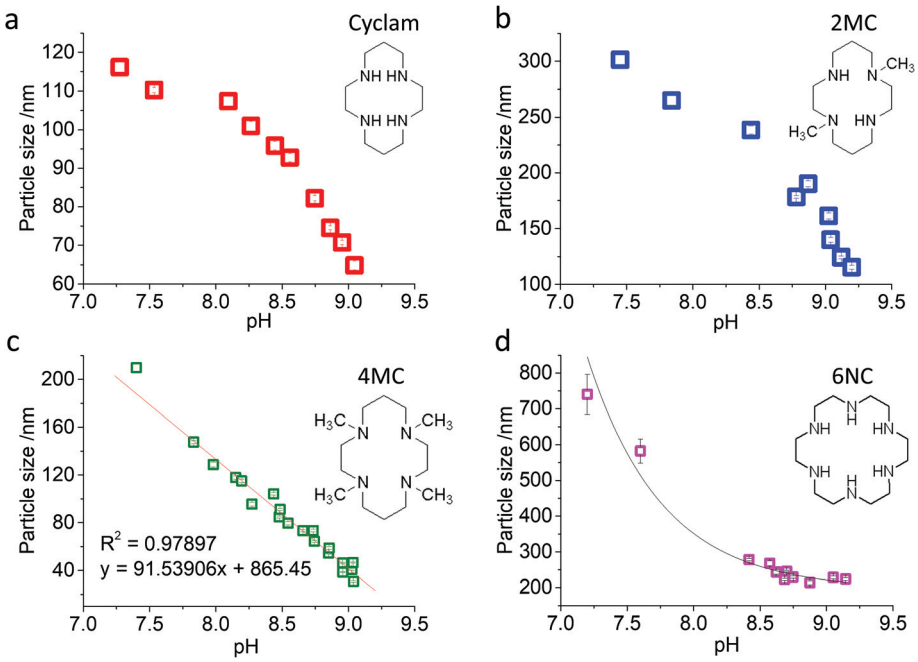

Fig. 8 The effect of azamacrocycle identity on silica sol formation. Si : N ratio of 1 : 1.

due to the low level of retention of the molecules with the silica phase formed.

In contrast to the two common routes to monodisperse silicas which differ in their use of acetic acid (Karmaker)[34] or ammonia (Stöber)[35] to catalyse the formation of silica, and take many hours to complete, our approach is significantly quicker. Materials prepared in the presence of several of the azamacrocyles tested retain very little organic material meaning that the remaining, unbound additive could be recycled using a recently patented approach.[36] Further detailed studies are required to understand the limitations of the approach and the mechanism of particle formation. These are beyond the scope of the current contribution and may take considerable time to unpick as shown by the vast literature on the Stöber process, the first major paper being reported in 1968 and only in 2017 was an article published 'unravelling the growth mechanism of silica particles in the Stöber method'.[37]

Conclusion

We have shown that the azamacrocycle 'cyclam' can be used to generate novel crystalline materials that exhibit a hollow tetragonal tube-like macrostructure, whose dimensions can be tuned according to the pH of the synthesis medium. The synthesis approach was successful for both silicon and germanium and we hypothesise that a range of other catecholate precursors of elements such as iron could be used to generate a large array of inorganic materials with interesting morphologies. The synthesis approach can be extended to tertiary diamines with functional group spacing playing an important role in the efficacy of complexation. Of the molecules explored to date, a C2 spacing leads to the most efficient structure control. In addition, we show that azamacrocycles can be used to manipulate silica formation and provide a fast synthesis route to particle sizes whose diameter can be tuned from *ca.* 20 nm to several hundred nm under mildly basic pH, conditions that will be suitable for their direct use in biotechnological applications.

Materials and methods

Materials

All chemicals were purchased from Sigma Aldrich and used without further purification unless otherwise stated. These included silicon and germanium containing precursors (dipotassium tris(1,2-benzenediolato-*O*,*O*′)silicate (KSiCat), tetramethoxysilane) (TMOS) and dipotassium tris(1,2-benzenediolato-*O*,*O*′)germanate 97% (KGeCat), cyclic compounds containing heteroatoms (1,4,7-triazacyclononane (3NC), 1,4,7,10-tetraazacyclododecane (4N2), 1,4,8,11-tetraazacyclodecane (cyclam), 1,8-dimethyl 1,4,8,11-tetraazacyclodecane (2MC), 1,4,8,11-tetra methyl 1,4,8,11-tetraazacyclodecane (4MC), 1,4,7,10,13,16-hexaazacyclooctadecane (6NC). 12-Crown-4 (12C4), 18-crown-6 (18C6)), amines: (*N*,*N*′-bis(3-aminopropyl)-1,3-propanediamine, *N*,*N*′-dimethyl-1,6-hexanediamine, tris(dimethylamino) methane, 1,1,4,7,10,10-hexamethyltriethylenetetramine, 3,3′-iminobis(*N*,*N*-dimethylpropylamine), 1,3-diamino-2-hydroxypropane-*N*,*N*,*N*′,*N*′-tetraacetic acid, 3-(dimethylamino)-1-propylamine, *N*,*N*,*N*′,*N*′-tetramethyldiaminomethane, *N*,*N*,*N*′,*N*′-tetramethylethylenediamine (4MEDAE), *N*,*N*,*N*′,*N*′-tetramethyl-1,4-butanediamine (4METAB), *N*,*N*,*N*′,*N*′-tetramethyl-1,6-hexanediamine (4MEDAH), *N*,*N*,*N*′,*N*″,*N*″-pentamethyldiethylenetriamine, *N*,*N*,*N*′-trimethyl-1,3-propanediamine, *N*,*N*,*N*′-trimethylethylenediamine. The silicon catecholate complex was purified to >99% by recrystallising from methanol with purity assessed by ^{1}H NMR (Jeol ECX-400 spectrometer) and a molybdenum blue assay.[38] The charge speciation diagrams for important cyclic compounds and amines was calculated using SPARC.[32] The starting concentration of silica/germania precursors was 30 mM throughout unless otherwise stated.

Synthesis of crystalline inorganic–organic hybrid materials

Materials were prepared by mixing the silicon catecholate with either azamacrocyclic compounds or diamines at Si : N ratios from 10 : 1 through to 1 : 1 and a range of pH (adjusted using acid or base but always above the pH where decomposition of the catecholate complex to orthosilicic acid occurs at around *ca.* pH 6.5) with the azamacrocyclic maintained at the same pH.

An example synthesis follows: KSiCat (0.14 g (30 mM)) was dissolved in 7.76 mL of distilled and deionised ice-cold water (dd water) to give a 30 mM solution on completion of addition of all components. A solution of cyclam (2 mL) was prepared in ice cold dd water at a Si : N ratio of 10 : 1 (0.0015 g, 7.5 μM). Acid, 2 M HCl (240 μL) to generate the desired pH was added to the cyclam solution. The two solutions were mixed and kept at room temperature or 5 °C, the pH was taken after 15 minutes and the precipitate isolated by centrifugation after 60 minutes, unless otherwise stated. The precipitate was washed with dd water (40 mL) followed by centrifugation 3 times and the material lyophilised (Virtis freeze dryer). For materials prepared at a range of pH values, acid was added to both solutions to give the desired pH (after 15 minutes) and the solutions then mixed. The same procedure was used to make materials using dipotassium tris(1,2-benzenediolato-*O*,*O*′)germanate (KGeCat) as a starting material and for materials prepared with 4MEDAE, 4MEDAB and 4MEDAH.

Materials characterisation

Samples were investigated using Thermal Gravimetric Analysis (TGA) using a PerkinElmer Pyris 6 TGA. The samples were heated at 10 °C min^{-1} from 30 to 900 °C in air to ensure complete combustion of organic material retained within the material. FTIR was performed using Nicolet Magna IR-750 spectrometer fitted with a Golden Gate attenuated total reflection (ATR) accessory (Thermo Nicolet). Spectra were recorded at 4 cm^{-1} resolution, averaging 64 scans. Powder X-ray diffraction was performed using a Hilton Brooks modified Philips PW1050 powder diffractometer operating at 42.5 kV/18 mA

with a copper source Cu Kα = 1.540562 Å. Scans were performed in step mode with 0.02θ step size and 0.2 s dwell time. Data were recorded over the 2 range 3–80θ at room temperature. Single crystal X-ray diffraction measurements were performed in Experimental Hutch 1 (EH1) of Beamline I19, at Diamond Light Source.[39] The data were collected at a wavelength of 0.6889 Å on a Fluid Film Devices 3-circle fixed-chi diffractometer using a Dectris Pilatus 2M detector. The crystal was mounted on a MiTeGen micromount using a perfluoropolyether oil and cooled for data collection by a Cryostream nitrogen-gas stream.[40] The collected frames were integrated using XIA2 [41–45] software and the data were corrected for absorption effects using AIMLESS,[46] an empirical method.

All non-H atoms were located using direct methods and difference Fourier syntheses. Hydrogen atoms were placed and refined using a geometric riding model. All fully occupied non-H atoms were refined with anisotropic displacement parameters, unless otherwise specified. Crystal structures were solved and refined using the Olex2 software package[47] with SHELXL[48] (structure refinement) and SHELXT[49] (structure solution). CIF files were checked using checkCIF,[50] CCDC 1916071‡ contains the supplementary data for $[(C_6H_4O_2)_3Si][C_{10}H_{26}N_4]\cdot H_2O$.

Solid state NMR (^{13}C and ^{29}Si) was carried out at Durham University. A solid-state silicon-29 NMR spectrum was obtained at 59.56 MHz using a Varian Unity Plus spectrometer. It was recorded using cross polarisation with a 5 s recycle delay, 5 ms contact time and at a spin-rate of 5 kHz. Spectral referencing was with respect to external, neat tetramethylsilane. A solid state 13-carbon NMR spectrum was obtained at 125.66 MHz using a Chemagnetics Infinity 500 instrument. It was recorded with a 5 s recycle delay, a 1 ms contact time and spin-rate of 7 kHz. Spectral referencing was with respect to external, neat tetramethylsilane. CHN analysis was conducted at London Metropolitan University.

Silica sphere synthesis using azamacrocyclic compounds

The first stage involved a study of the effect of a series of azamacrocyclic compounds on silica condensation at pH 6.8 using a 30 mM TMOS condensing system where the silicon : nitrogen (Si : N) ratio was 10 : 1 or 1 : 1. A 1 M TMOS solution was prehydrolysed in 1 mM HCl for 15 minutes and then neutralised to the desired reaction pH (and concentration) in one step with additives being added during the neutralising step. The kinetics of the TMOS system were measured by taking 10 μL portions of the condensing solution at predetermined time intervals into a solution of 16.5 mL of molybdic acid solution forming silicomolybdic acid, which after 15 minutes was reduced to silicomolybdous acid[38] and absorbance at 810 nm measured after 24 hours. Data were treated[51] to calculate rate constants for the early stages of condensation. The formation of particles was followed using dynamic light scattering (DLS) (Malvern Zetasizer NanoS at 25 °C) operating in z-average mode. For azamacrocylics that increased the rate of condensation and showed stable DLS traces further reactions were performed over a range of pH values with data being reported for the pH ranges over which monodisperse silica sols were formed.

Conflicts of interest

There are no conflicts to declare.

Acknowledgements

NMR spectra were recorded at the solid-state NMR Service in Durham. We acknowledge Diamond Light Source for time on beamline I19 and beamline scientist Sarah Barnett under proposal CY21755. We also thank Alex Slawin of Edinburgh University for preliminary X-ray data and colleagues at NTU who attempted to generate single crystal X-ray data.

Funding is acknowledged from AFOSR FA9550-06-1-0154 and FA9550-16-1-0213.

References

1 P. D. Beer, *Acc. Chem. Res.*, 1998, **31**, 71–80.
2 P. D. Beer, *Chem. Soc. Rev.*, 1989, **18**, 409–450.
3 I. Lukes, J. Kotek, P. Vojtisek and P. Hermann, *Coord. Chem. Rev.*, 2001, **216**, 287–312.
4 S. Aime, M. Botta, M. Fasano and E. Terreno, *Chem. Soc. Rev.*, 1998, **27**, 19–29.
5 D. S. Wragg, G. B. Hix and R. E. Morris, *J. Am. Chem. Soc.*, 1998, **120**, 6822–6823.
6 T. Wessels, L. B. McCusker, C. Baerlocher, P. Reinert and J. Patarin, *Microporous Mesoporous Mater.*, 1998, **23**, 67–77.
7 P. S. Wheatley and R. E. Morris, *J. Solid State Chem.*, 2002, **167**, 267–273.
8 V. Patinec, P. A. Wright, P. Lightfoot, R. A. Aitken and P. A. Cox, *J. Chem. Soc., Dalton Trans.*, 1999, 3909–3911.
9 D. S. Wragg, A. M. Z. Slawin and R. E. Morris, *J. Mater. Chem.*, 2001, **11**, 1850–1857.
10 P. A. Wright, M. J. Maple, A. M. Z. Slawin, V. Patinec, R. A. Aitken, S. Welsh and P. A. Cox, *J. Chem. Soc., Dalton Trans.*, 2000, **8**, 1243–1248.
11 M. J. Maple, E. F. Philp, A. M. Z. Slawin, P. Lightfoot, P. A. Cox and P. A. Wright, *J. Mater. Chem.*, 2001, **11**, 98–104.
12 F. Serpaggi, T. Loiseau, F. Taulelle and G. Ferey, *Microporous Mesoporous Mater.*, 1998, **20**, 197–206.
13 S. Mann and G. A. Ozin, *Nature*, 1996, **382**, 313–318.
14 M. Sumper and N. Kröger, *J. Mater. Chem.*, 2004, **14**, 2059–2065.
15 H. A. Currie and C. C. Perry, *Ann. Bot.*, 2007, **100**, 1383–1389.
16 S. V. Patwardhan, *Chem. Commun.*, 2011, 7567–7582.
17 M. J. Limo, A. Sola-Rabada, E. Boix, V. Thota, Z. C. Westcott, V. Puddu and C. C. Perry, *Chem. Rev.*, 2018, 11118–11193.

18 M. R. Knecht and D. W. Wright, *Chem. Commun.*, 2003, 3038–3039.
19 D. J. Belton, S. V. Patwardhan and C. C. Perry, *Chem. Commun.*, 2005, 3475–3477.
20 D. J. Belton, S. V. Patwardhan and C. C. Perry, *J. Mater. Chem.*, 2005, **15**, 4629–4638.
21 V. V. Annenkov, S. V. Patwardhan, D. J. Belton, E. N. Danilovtseva and C. C. Perry, *Chem. Commun.*, 2006, 1521–1523.
22 P. J. Lopez, C. Gautier, J. Livage and T. Coradin, *Curr. Nanosci.*, 2005, **1**, 73–83.
23 D. J. Belton, S. V. Patwardhan, V. V. Annenkov, E. N. Danilovtseva and C. C. Perry, *Proc. Natl. Acad. Sci. U. S. A.*, 2008, **105**, 5963–5968.
24 M. M. Tomczak, D. D. Glawe, L. F. Drummy, C. G. Lawrence, M. O. Stone, C. C. Perry, D. J. Pochan, T. J. Deming and R. R. Naik, *J. Am. Chem. Soc.*, 2005, **127**, 12577–12582.
25 S. V. Patwardhan, R. Maheshwari, N. Mukherjee, K. L. Kiick and S. J. Clarson, *Biomacromolecules*, 2006, **7**, 491–497.
26 J. J. Yuan, P. X. Zhu, N. Fukazawa and R. H. Jin, *Adv. Funct. Mater.*, 2006, **16**, 2205–2212.
27 C. Gautier, P. J. Lopez, M. Hemadi, J. Livage and T. Coradin, *Langmuir*, 2006, **22**, 9092–9095.
28 J. J. E. Moreau, L. Vellutini, M. W. C. Man and C. Bied, *Chem. – Eur. J.*, 2003, **9**, 1594–1599.
29 P. Bindu, B. Varghese and M. N. Sudheendra Rao, *Phosphorus, Sulfur Silicon Relat. Elem.*, 2010, **178**, 2373–2386.
30 J. V. Kingston, B. Vargheese and M. N. Sudheendra Rao, *Main Group Chem.*, 2000, **3**, 79–90.
31 D. Sackerer and G. Nagorsen, *Z. Anorg. Chem.*, 1977, **437**, 188–192.
32 S. W. Karickhoff, L. A. Carreira and S. H. Hilal, *SPARC Performs Automated Reasoning in Chemistry*, 3.01 edn, University of Georgia.
33 R. D. Hancock, R. J. Motekaitis, J. Mashishi, I. Cukrowski, J. H. Reibenspies and A. E. Martell, *J. Chem. Soc., Perkin Trans. 2*, 1996, 1925–1929.
34 B. Karmaker, G. De, D. Kundu and D. Ganguli, *J. Non-Cryst. Solids*, 1991, **135**, 29–36.
35 W. Stöber, A. Fink and E. Bohn, *J. Colloid Interface Sci.*, 1968, **26**, 62–69.
36 J. R. H. Manning and S. V. Patwardhan, *US Patent App*. 15/757182, 2018.
37 Y. Han, Z. Lu, Z. Teng, J. Liang, Z. Guo, D. Wang, M.-Y. Han and W. Yang, *Langmuir*, 2017, **33**, 5879–5890.
38 D. J. Belton, O. Deschaume, S. V. Patwardhan and C. C. Perry, *J. Phys. Chem. B*, 2010, **114**, 9947–9955.
39 D. R. Allan, H. Nowell, S. A. Barnett, M. R. Warren, A. Wilcox, J. Christensen, L. K. Saunders, A. Peach, M. T. Hooper, L. Zaja, S. Patel, L. Cahill, R. Marshall, S. Trimnell, A. J. Foster, T. Bates, S. Lay, M. A. Williams, P. V. Hathaway, G. Winter, M. Gerstel and R. W. Wooley, *Crystals*, 2017, **7**, 336.
40 J. Cosier and A. M. Glazer, *J. Appl. Crystallogr.*, 1986, **19**, 105–107.
41 P. Evans, *Acta Crystallogr., Sect. D: Struct. Biol.*, 2006, **62**, 72–82.
42 G. Winter, *J. Appl. Crystallogr.*, 2010, **43**, 186–190.
43 P. R. Evans and G. N. Murshudov, *Acta Crystallogr., Sect. D: Struct. Biol.*, 2013, **69**, 1204–1214.
44 G. Winter, D. G. Waterman, J. M. Parkhurst, A. S. Brewster, R. J. Gildea, M. Gerstel, L. Fuentes-Montero, M. Vollmar, T. Michels-Clark, I. D. Young, N. K. Sauter and G. Evans, *Acta Crystallogr., Sect. D: Struct. Biol.*, 2018, **74**, 85–97.
45 M. D. Winn, *et al.*, *Acta Crystallogr., Sect. D: Struct. Biol.*, 2011, **67**, 235–242.
46 CCP4 2018, 7.0.072: AIMLESS version 0.7.4 : 13/12/18.
47 (*a*) O. V. Dolomanov, L. J. Bourhis, R. J. Gildea, J. A. K. Howard and H. Puschmann, *J. Appl. Crystallogr.*, 2009, **42**, 339–341; (*b*) O. V. Dolomanov, A. J. Blake, N. R. Champness and M. Schroder, *J. Appl. Crystallogr.*, 2003, **36**, 1283–1284.
48 G. M. Sheldrick, *Acta Crystallogr., Sect. C: Struct. Chem.*, 2015, **71**, 3–8.
49 G. M. Sheldrick, *Acta Crystallogr., Sect. A: Found. Crystallogr.*, 2015, **71**, 3–8.
50 http://checkcif.iucr.org.
51 C. C. Harrison (now Perry) and N. Loton, *J. Chem. Soc., Faraday Trans.*, 1995, **91**, 4287–4297.

